IBRO Neuroscience Reports 13 (2022) 243–254

Contents lists available at ScienceDirect

IBRO Neuroscience Reports

journal homepage: www.sciencedirect.com/journal/IBRO-Neuroscience-Reports

Neural recovery after cortical injury: Effects of MSC derived extracellular vesicles on motor circuit remodeling in rhesus monkeys

Samantha Calderazzo [a,*], Margaret Covert [a], Diego De Alba [a], Bethany E. Bowley [a], Monica A. Pessina [a], Douglas L. Rosene [a,b], Benjamin Buller [c], Maria Medalla [a,b,1], Tara L. Moore [a,b,1]

[a] Anatomy and Neurobiology Dept, BUSM, USA
[b] Center for Systems Neuroscience, BU, USA
[c] Henry Ford Health Care System, USA

ARTICLE INFO

Keywords:
Ischemia
Cortical Injury
Extracellular Vesicles
Stem Cell-Based Treatments
Motor Cortex
Circuit Remodeling
Plasticity

ABSTRACT

Reorganization of motor circuits in the cortex and corticospinal tract are thought to underlie functional recovery after cortical injury, but the mechanisms of neural plasticity that could be therapeutic targets remain unclear. Recent work from our group have shown that systemic treatment with mesenchymal stem cell derived (MSCd) extracellular vesicles (EVs) administered after cortical damage to the primary motor cortex (M1) of rhesus monkeys resulted in a robust recovery of fine motor function and reduced chronic inflammation. Here, we used immunohistochemistry for cfos, an activity-dependent intermediate early gene, to label task-related neurons in the surviving primary motor and premotor cortices, and markers of axonal and synaptic plasticity in the spinal cord. Compared to vehicle, EV treatment was associated with a greater density of cfos^{+} pyramidal neurons in the deep layers of M1, greater density of cfos^{+} inhibitory interneurons in premotor areas, and lower density of synapses on MAP2+ lower motor neurons in the cervical spinal cord. These data suggest that the anti-inflammatory effects of EVs may reduce injury-related upper motor neuron damage and hyperexcitability, as well as aberrant compensatory re-organization in the cervical spinal cord to improve motor function.

Introduction

Every year, over 795,000 people in the United States experience a stroke, of which 140,000 will die while many of the survivors suffer long-term disability (AHA stroke.org; Benjamin et al., 2017). However, the only FDA approved stroke therapies target removal of blood clots to re-perfuse brain tissue during the acute post-stroke phase (Koroshetz, 1996; Leon-Jimenez et al., 2014; Saver et al., 2013). Other than physical rehabilitation, there are no effective treatments to facilitate recovery (Grefkes and Ward, 2014) and a full return of function rarely occurs in humans. Therefore, new therapeutic agents are critically needed to reduce overall damage following a stroke and enhance re-organization.

After cortical injury, there is an increase in oxidative stress and pro-inflammatory processes leading to apoptosis within the lesion (Lipton, 1999) and hyperexcitability of surviving neurons in the surrounding areas (Carmichael, 2012; Kohman and Rhodes, 2013; Lai et al., 2014; Jayaraj et al., 2019). We and others have reported that stem cell-based therapies reduce inflammation and neuronal damage while enhancing plasticity after cortical injury (Chopp, et al., 2009; Lakhan et al., 2009; Mahmood, et al., 2005; Stonesifer et al., 2017; Liu et al., 2010; Lambertsen, et al., 2018; Orczykowski et al., 2018; Go et al., 2020). In particular, mesenchymal stem cells (MSC) release endosome derived microvesicles, known as extracellular vesicles (EVs). MSC derived EVs (MSCdEVs) contain microRNAs (miRNA) and proteins that can penetrate the blood brain barrier (Matsumoto et al., 2017; Banks et al., 2020) and appear to promote functional recovery, anti-inflammatory responses, and plasticity in rodent models (Katakowski et al., 2013; Xin et al., 2012; Aleynik et al., 2014; Marei et al., 2018; Di Trapani et al.,

Abbreviations: CSC, Cervical Spinal Cord; CR, Calretinin; CB, Calbindin; DH, Dorsal Horn; dPMC, dorsal Premotor Cortex; EVs, Extracellular Vesicles; LCST, Lateral Corticospinal Tract; M1, Primary Motor Cortex; MAP2, Microtubule Associated Protein 2; miRNA, Micro RNA; MSCd, Mesenchymal Stem Cell derived; NHP, Non-Human Primate; PV, Parvalbumin; periM1, Perilesional Primary Motor Cortex; ROS, Reactive Oxygen Species; SYN, Synaptophysin; VH, Ventral Horn.

* Corresponding author.
E-mail address: scaldera@bu.edu (S. Calderazzo).
[1] Co-senior Authors

https://doi.org/10.1016/j.ibneur.2022.08.001
Received 11 February 2022; Received in revised form 1 July 2022; Accepted 7 August 2022
Available online 18 August 2022

2016; Phinney et al., 2017; B. Zhang et al., 2014, 2016). We further tested the efficacy of these MSCs derived EVs in our non-human primate (NHP) model of cortical damage, which resulted in significant functional recovery within the first few weeks after the injury (Moore et al., 2019). Further, this EV-mediated enhanced recovery is associated with an increase in ramified surveying microglia (Go et al., 2020), and myelin maintenance (Go et al., 2021), as well as preservation of excitatory: inhibitory (E:I) balance within pyramidal neurons (Medalla & Chang et al., 2020). Yet, it is unknown how this functional recovery relates to neuronal laminar cortico-cortical and cortico-spinal motor circuitry.

Studies have shown that compensatory activation of premotor cortices (PMC) and their spinal cord projections help support motor recovery after injury in M1 (Barbas and Pandaya 1987; Johansen-Berg et al., 2002; Kantak et al. 2012; Morecraft et al., 2019). Specifically, recruitment of activity from the premotor areas can occur after injury (Johansen-Berg et al., 2002; Carmichael, 2003; Dancause et al., 2005; Carmichael, 2006; Darling et al., 2011; Nishimura and Isa, 2012) to compensate for lost signals. However, pre-motor hyperactivation needs to be properly regulated otherwise hyper-excitability and glutamate toxicity can further damages neurons (Carmichael, 2012; Kohman and Rhodes, 2013; Lai et al., 2014; Jayaraj et al., 2019). Additionally, corticospinal projections of motor cortices sprout new connections in the spinal cord to compensate for damaged M1 projections and re-innervate lower motors neurons (LMN) (Wiessner et al., 2003; Weidner et al., 2001; Lee et al., 2004; Zai et al., 2009). Yet, new compensatory synaptic connections also need to be tightly controlled as aberrant neuronal plasticity after injury associates with functional impairments (Niv et al., 2012; Kim et al., 2015; Beauparlant et al., 2013; Wahl et al., 2014; Gennaro et al., 2017) and prevention of this abnormal plasticity after stroke can improve recovery (Cuartero et al., 2019).

cfos is an activity dependent early intermediate gene upregulated after depolarization (Morgan et al., 1987; Saffen et al., 1988; Link et al., 1995; Lyford et al., 1995) and can label recently active neurons following a sustained behavioral task (Guzowski et al., 1999; Vann et al., 2000; Hall et al., 2001; Ramirez-Amaya et al., 2005). Our recent work in the ventral PMC (Medalla & Chang et al., 2020) reports increases in $cfos^{+}$ activation of calbindin-positive (CB^{+}) inhibitory neurons with MSCd EVs. However, whether distinct layers and motor cortical areas exhibit cell-type specific $cfos^{+}$ activation to support compensatory activity for recovery of function after injury is unknown. The relevance of cortical layers is that they give rise to distinct cortical and cortico-spinal connections, which play different roles in motor control (Morecraft et al., 2019), and likely have selective vulnerability to injury. Building on this, we have now assessed the functional remapping of laminar cortical and spinal motor circuits after injury and treatment with MSCd-EVs. Specifically, we quantified layer specific neuronal numbers and activity via cfos labeling in the perilesional M1 cortex (periM1) and dorsal premotor cortices (dPMC), along with markers for synaptic plasticity in the cervical spinal cord. Here we provide evidence that EV treatment resulted in greater pyramidal neuron cfos+ activity in the periM1 and reduced presumably aberrant synapses in the ventral horn (VH) of the cervical spinal cord (CSC) compared to vehicle treatment. Additionally, EV treatment promoted inhibitory neuron activity in the dPMC, likely downregulating injury-related compensatory hyperexcitability.

Methods

Subjects

Ten female rhesus monkeys (Macaca mulatta) ranging from 16 to 26 years of age (approximately equivalent to 48- and 78-year-old humans; Tigges et al., 1988) were obtained from the National Primate Research Facilities or Private Vendors and had known birthdates with complete health records (Table 1). Monkeys received medical examinations and magnetic resonance imaging to ensure there was no occult health problems or neurological damage. Monkeys were housed in the Animal Science Center of Boston University School of Medicine which is AAALAC accredited. All procedures were approved by the Boston University Institutional Animal Care and Use Committee.

Table 1
Subject List. Details on subjects used for this study. There were 5 females in each treatment group with no significant differences in age or weight between groups.

Animal	Group	Age	Weight	Sex
AM320	EVs	21.83	11.4	F
AM332	EVs	24.08	12.1	F
AM338	EVs	16.42	6.1	F
SM061	EVs	21.75	6.2	F
SM062	EVs	20.92	8.2	F
Mean		21.00 (+/- 1.26)	8.80 (+/- 1.27)	
AM323	Vehicle	23.67	11	F
AM331	Vehicle	26.08	13.1	F
AM335	Vehicle	20.33	9.5	F
AM337	Vehicle	24.33	7	F
AM339	Vehicle	21.42	10.3	F
Mean		23.17 (+/- 1.02)	10.18 (+/- 0.99)	
Ttest		P = 0.109	P = 0.208	

Cortical Injury

All surgical procedures were carried out under aseptic conditions following the description in Moore et al., 2019. Each monkey was anesthetized with intravenous sodium pentobarbital (15–25 mg/kg) to effect, and antibiotics and analgesics were given prior to and following surgery. To create reproducible cortical injury and motor deficits, the precentral gyrus was systematically explored using electrical stimulation while a trained observer noted muscle movements in specific areas of the digits, hand, forearm or arm, both visually and by palpation. Electrophysiological stimulation was used to create a cortical surface map of the hand area that was used to guide placement of the lesion. Cortical injury was induced as described in Moore et al., 2019 via a small glass suction pipette that was inserted under the pia and used to bluntly transect the small penetrating arterioles. Suction and irrigation with sterile saline were sufficient to stanch bleeding and maintain a clear field. This pial dissection of penetrating vessels removes the blood supply to the cortex of the hand representation, inducing degeneration that extends down to the underlying white matter. Immediately following surgery and for 3–7 days post-op, antibiotics and analgesics were administered. As previously reported (Moore et al., 2019; Go et al., 2020) an independent samples Student's T-test comparing the volume of the lesion between the vehicle control and treated monkeys revealed no significant differences between groups (T = –0.732, P = 0.488).

Motor Testing

As described in detail previously (Moore et al., 2010; Moore et al., 2016), monkeys were tested on a task of fine motor function of the hand, the Hand Dexterity Task (HDT), using a testing apparatus that controls, quantifies, and video records responses from each hand. Monkeys were trained pre-operatively to asymptotic performance with equal trials to both hands and lesions were made in the cortex controlling the preferred hand. Postoperative re-testing began two weeks after surgery and continued for 12 weeks. Seventy percent of the trials required the use of the impaired hand, which is similar to the constraint-induced therapy that is frequently used in human rehabilitation (Corbetta et al., 2015; Kwakkel et al., 2016; Souza et al. 2015). The length of time required for monkeys to achieve asymptotic or pre-operative function was recorded. The criterion on this task for successful return to pre-operative performance was five consecutive days at or below the pre-operative time to retrieve the food reward.

Final Testing and cfos activation: On the day of euthanasia at 14 weeks post-injury, monkeys were tested on the HDT task for 1 h. For this final

testing session all trials were administered to the impaired hand to maximize activation of neurons participating in function of the impaired hand. Two hours after the completion of the final testing session, monkeys were euthanized, an interval sufficient to allow expression of the cfos protein in activated neurons. (Zhong et al. 2014; Barros et al., 2015).

Grasp assessment

We used video recordings of the pre- and post-operative performance on the HDT and our Non-Human Primate Grasp Assessment Scale (GRAS) to quantify impairments and recovery of fine motor function of the hand. Using the GRAS, we evaluate recovery of function of individual digits and precise finger-thumb pinch to distinguish between compensatory grasp function and a return to pre-injury grasp patterns (Pessina et al., 2019).

Extracellular vesicle preparation and administration

EVs were extracted from MSCs harvested from the bone marrow of one young adult monkey as detailed in Moore et al., 2019. The EVs given to all animals in this study came from the same bone marrow sample and MSC extraction batch and therefore should be identical in content. Treatments were prepared at a concentration of 4×10^{11} particles/kg in 10 mL of PBS via an Izon qNano particle counter. Monkeys received the treatment or a PBS vehicle intravenously at 24 h and 14 days post injury. Dosing was determined based on our rodent studies (Xin, Li, Cui, et al., 2013; Y. Zhang et al., 2017). Dosing intervals were based on the rodent studies 24 h administration. However, we chose to also administer a second dose of EVs at 14 days since larger animals have a slower neural recovery (Agoston, 2017) and based on previous experience with functional improvements in our rhesus monkey model.

Tissue collection and preparation

Brain and cervical spinal cord (CSC) were collected at 14 weeks post-injury following 12 weeks of behavioral testing. For perfusion-fixation, monkeys were sedated with Ketamine (10 mg/kg IM) deeply anesthetized with sodium pentobarbital (25 mg/kg IV to effect) and were euthanized by exsanguination during transcardial perfusion-fixation of the CNS. The brain was blocked, in situ, in the coronal plane and removed from the skull. The CSC was removed from the vertebral column and cut with a 45-degree angle to denote rostral from caudal and notched on the ipsilesional side for later processing. Tissue was post-fixed overnight in 4% paraformaldehyde and then transferred to cryoprotectant solution. Cryoprotected blocks were flash frozen at − 75 °C and stored at − 80 °C. Frozen sections were cut on a sliding microtome while frozen in dry ice into interrupted series of coronal sections (10 series of 30 μm thick sections) with a 300 μm spacing between sections. Sections were collected in phosphate buffer with 15% glycerol and stored at − 80 °C. Spinal cord tissue processed in the same way but cut into interrupted series of transverse sections (12 series of 40 μm thick sections) with a 480 μm spacing between sections. Sections were collected in phosphate buffer with glycerol and 30% sucrose stored at − 20 degrees.

Immunohistochemistry

Antibodies labeling synapses, dendrites, axons, neuron activation, inhibitory interneurons, and pyramidal neurons were used to assess CNS tissue. Microtubule associated protein 2 (MAP2) was used to label lower motor neurons and their associated dendrites. Synaptophysin (SYN) is a presynaptic integral membrane glycoprotein used to label synapses. Neurofilament (clone:SMI32) and calcium binding proteins calretinin (CR), parvalbumin (PV) and calbindin (CR) were used to label subpopulations of pyramidal neurons and inhibitory interneurons, while cfos labeled neuronal nuclei of cells that were active during recent behavioral tasks. All assays were batched processed and simultaneously thawed to room temperature.

Fluorescence

For immunofluorescence, sections were incubated in a blocking solution of 10% normal goat serum (NGS), 1 M glycine, and 0.4% triton for two hours and then incubated in the appropriate primary antibodies (1:500 MAP2 abcam; 1:500 SYN abcam; 1:400 cfos Synaptic Systems; 1:1000 PV; 1:1000 CB Swant; 1:2000 CR Swant) overnight at room temperature. The next day tissue was rinsed and incubated with the corresponding secondary antibodies (1:600; Alexa Fluor Invitrogen or Jackson Immunoresearch) in the dark for two hours. Sections were mounted on glass slides and cover-slipped with Prolong anti-fade medium (Life Technologies) and left at room temperature in the dark for 36 h before being imaged. Control experiments where the primary antibody was omitted showed no labeling.

Brightfield

Double labeled chromogen sections were sequentially run 1 label at a time. First sections were exposed to 3% hydrogen peroxide for 30 min, followed by a 1 h 10% NGS block and overnight primary antibody incubation (1:1000 SMI32 or 1:1000 cfos). The next day sections were incubated with the corresponding biotinylated secondary antibodies (Vector) for 1 h followed by a 1-hour amplification step (ABC Elite, Vector) and exposure to enzyme mediated color reactions. For the second label sections were rinsed and incubated in Superblock (Thermofisher) for 1 h. Antibody, amplification, and enzyme steps were repeated for the second label.

Data analysis

Brightfield cell counts

Cell density was assessed in the perilesional M1 cortex (periM1) as well as the dorsal premotor cortex (dPMC) on the ipsilesional hemisphere using the optical fractionator probe of Stereoinvestigator (MBF Bioscience) (Fig. 1B,C). Pyramidal neurons ($SMI32^+$), active pyramidal neurons ($SMI32^+cfos^+$ cells), or other active neurons ($SMI32^-cfos^+$) (Fig. 2B) were counted using 3–5 sections per monkey and the sampling scheme was optimized based on Gundersen's Coefficient of Error (<0.1). Unfortunately, cortical injury made the upper layers very difficult to define in the periM1 (Fig. 1E), hence we only counted deep (4−6) layers. However, in the dPMC counts were segregated by upper (1−3) layers and deep (4−6) layers.

Fluorescent cell counts

To estimate the density of $cfos^+$ neurons co-labeled with inhibitory markers (CB, PV or CR), 4-channel confocal image stacks were acquired (Zeiss 710; 20x, 0.8 N.A; 0.3 ×0.3 ×1 μm voxel). From each monkey, 8 fields, spaced 500 μm apart, in the upper (1−3) and deep (4−6) layers of the dPMC, were randomly selected and imaged throughout the entire z extent of two 30 μm section. In each z-stack, the cells single- and double-labeled with the markers of interest were counted using FIJI cell counter [(http://imagej.nih.gov/ij/, 1997–2016); RRID:SCR_003070; (Schindelin et al., 2012)]. Stereological counting rules were applied with inclusion and exclusion borders, as described by Fiala and Harris, (2001).

CSC analysis

FIJI software (National Institutes of Health) was used to analyze fluorescent images. To assess dendritic changes, the MAP2 channel was separated and z-projected onto a 2D plane. Background was subtracted

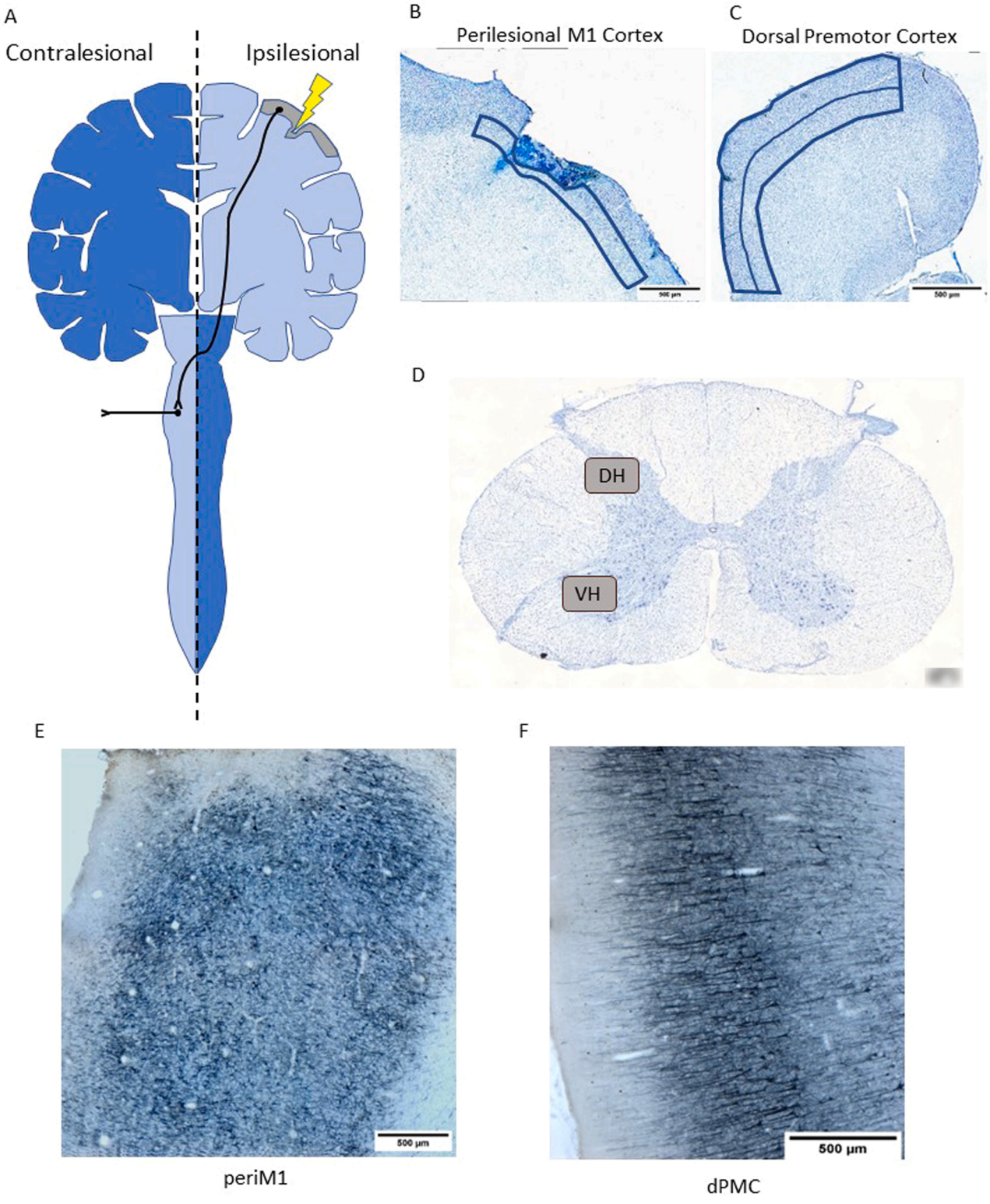

Fig. 1. Histological Methods: A) Schematic of experimental design and sampling areas. After lesioning the hand area of the motor cortex, we assessed whether extracellular vesicle (EV) treatment enhanced neuronal integrity and repair in the ipsilesional cortex and contralesional cervical spinal cord. B, C) Brightfield images of Nissl-stained coronal sections showing cortical ROIs, which include L5–6 of the perilesional cortex (periM1, B) and L1–6 of the dorsal premotor cortex (dPMC, C) separated into upper (L1–3) and deep layers (L4–6). D) Nissl-stained coronal sections showing cervical spinal cord ROIs including the Ventral Horn (VH), as well as the Dorsal Horn (DH) as a control region. E, F) Brightfield images showing dual labeling of SMI32 (blue) and cfos (brown, not readily distinguished at this objective). Note the disrupted layer architecture within the periM1 near the lesion (E), compared to dPMC (F) further way from the lesion. Scale bars 500 µm.

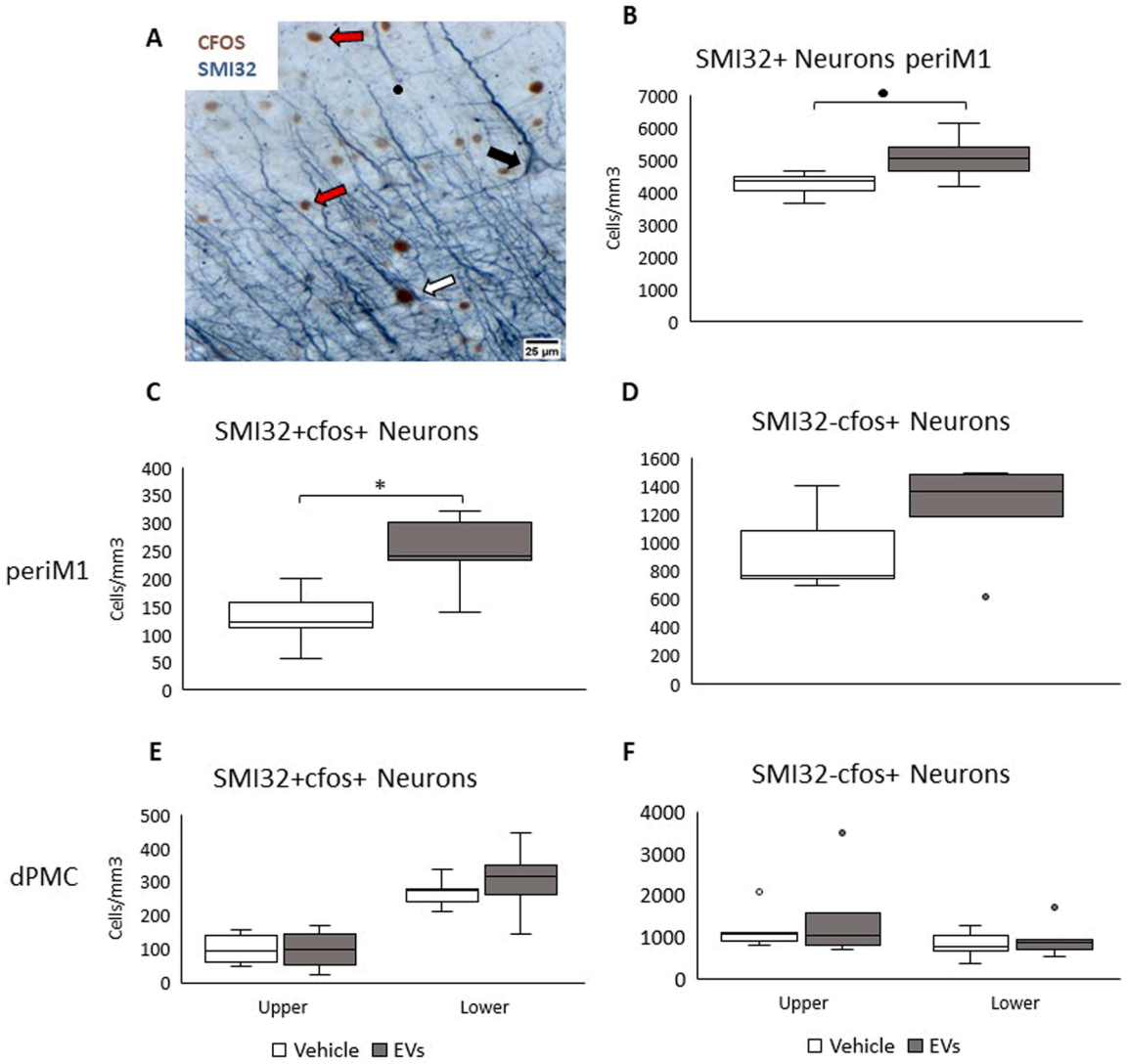

Fig. 2. MSCd-EV Effects on Task-relevant cfos^{+} Activation of Pyramidal Neurons in the Motor Cortices: **A**) Representative brightfield image of coronal section in dorsal premotor cortex (dPMC) showing dual labeling of SMI32 (blue) and cfos (brown). We analyzed the number of SMI32^{+} pyramidal neurons (black arrow; A) and SMI32^{+}cfos^{+} presumably task-activated pyramidal neurons (white arrow) as well as the number of SMI32-cfos^{+} task activated non-pyramidal neurons (red arrows). **B**) Box and whisker plots showing the density of SMI32^{+} neurons, **C**) the subset of double labeled SMI32^{+}cfos^{+} pyramidal neurons and **D**) double labeled SMI32-cfos^{+} neurons in periM1. **E**) Box and whisker plots showing the density of double labeled SMI32^{+}cfos^{+} pyramidal neurons and **F**) double labeled SMI32-cfos^{+} neurons in dPMC. Gray/White circles represent outliers on the graphs. Scale bar 25 µm.

and percent area assessed via FIJI measurement tools. We used MAP2 and SYN colocalization to estimate synaptic density along the dendritic shafts and somas of lower motor neurons as previously done (Skup et al., 2012; Maxwell et al., 2018; Lee et al., 2021). Briefly, co-labeled z-stacks of the VH and DH were split into two channels and run through the FIJI Coloc2 tool. Mander's colocalization coefficient (CLC) was used for analysis.

Statistics

R Studio was used to run all statistical analyses. Cell densities and proportion of active neuronal subtypes were run through mixed two-way ANOVAs comparing between factors "group" (untreated, treated) and within subject factors "layers" (upper, deep). periM1 densities were run through Student T-tests since only deep layers were counted. Percent area or CLCs from CSC images were run through a two-way mixed ANOVA with between factors "group" (treated, untreated) and within subject factor "hemisphere side" (ipsilesional, contralesional). Post Hoc Student T-tests with Bonferroni corrections were run when appropriate. Outliers were determined based on 1.5x the interquartile range. Removal of outliers did not significantly change any of the statistics so we did not remove them from the final analyses, but they are noted on the graphs. Additionally, all outcomes were analyzed through a multiple linear correlation model against grasp recovery endpoints (days to return to pre-operative grasp and mean grasp scores during the final week) and HDT latency endpoints (days to return to pre-operative latency and retrieval latency during the final week) to assess associations with measures of functional recovery.

Results

MSCd EVs increase the density of cfos activated pyramidal neurons in the periM1

We examined the density of pyramidal neurons marked by SMI32, a non-phosphorylated neurofilament protein enriched in L3 and L5 pyramidal neurons (Campbell and Morrison, 1989), in the periM1 directly below and surrounding the lesion, where the pia is not intact. In all

cases, the pia and upper layers L2–3 were not intact, thus pyramidal neurons were counted in L5–6 of periM1. Student T-test showed a trend of higher SMI32$^+$ neuron density in the deep periM1 layers in EV treated monkeys (T(9,1)= 2.186, P = 0.070; Fig. 2B). Using dual immuno-labeling (Fig. 2 A), we then assessed the density of SMI32$^+$ neurons expressing cfos, an intermediate early gene that is upregulated in task-related neurons, about 2 h after performing the motor task (Orczykowski et al., 2018). In the periM1, a Student T-test showed a significantly larger number of cfos activated SMI32 pyramidal neurons (SMI32$^+$cfos$^+$) in EV treated monkeys (T(9,1)= 2.50, P = 0.020; Fig. 2 C). Student T-test of SMI32$^-$cfos$^+$ neurons showed no significant difference between groups (T(9,1)= 1.361, P = 0.212; Fig. 2D). These data indicate a higher number and task-related activity of SMI32 pyramidal neurons in the periM1 of EV treated monkeys after cortical injury.

MSCd EVs decrease the density of cfos activated pyramidal neurons in the dPMC

Neurons in premotor cortices have been shown to exhibit compensatory hyperactivation after injury in M1 (Carmichael, 2012; Kohman and Rhodes, 2013; Lai et al., 2014; Jayaraj et al., 2019). To investigate whether damage in M1 resulted in compensatory changes in pyramidal neurons and task-related activation in premotor areas, we assessed the density of SMI32$^+$ and cfos$^+$ neurons in layers 2–3 and 5–6 of dorsal PMC (dPMC). Neurons in upper L2–3 of dPMC are one source of cortico-cortical projections to M1, while the deep L5–6 neurons contain subsets that project to the spinal cord and other subcortical structures (Dum and Strick, 1991). A two-way ANOVA revealed no difference in the number of SMI32$^+$ pyramidal neurons between groups (F(9,1)= 1.401, P = 0.256), no effect of layer (F(9,1)= 3.093, P = 0.10) and no interactions (F(9,1)= 0.519, P = 0.483). SMI32$^+$cfos$^+$, presumably task-activated pyramidal cells, show no significant differences between groups (F(9,1)= 3.31, P = 0.092; Fig. 2E), no effect of layer (F(9,1)= 2.171, P = 0.164) and no interactions (F(9,1)= 2.25, P = 0.158). SMI32$^-$cfos$^+$ neurons showed no significant difference between groups (F(9,1)= 1.03, P = 0.328; Fig. 2 F), or layers (F=0.216, P = 0.649) and no significant interaction (F(9,1)= 0.182, P = 0.676).

To further investigate the laminar distribution of these presumably task-activated neurons, we mapped the percent of cfos$^+$ active SMI32$^+$ and SMI32$^-$ neurons across upper and deep layers of the cortex. In both groups SMI32$^-$cfos$^+$ neurons show a higher concentration in the upper layers (Vehicle:59.5%, EVs:59.1%), while SMI32$^+$cfos$^+$ neurons show a high concentration in deep layers (Vehicle:71.1%, EVs:78.12%). A subset of these deep layer pyramidal neurons likely contributes to long-range cortico-subcortical motor projections, while neurons in the upper layer are either cortico-cortical projections or local inhibitory interneurons (Ralston et al., 1985; Dum and Strick, 1991, Hof et al., 1995; Morecraft et al., 2013, 2019). Hence, we further subtyped the active cfos$^+$ neurons.

MSCd EVs increase the density of cfos activated inhibitory interneurons in the dPMC

A cortical insult to the motor cortex, can result in hyperexcitability of the surviving motor and premotor neurons (Carmichael, 2012; Kohman and Rhodes, 2013; Lai et al., 2014; Jayaraj et al., 2019). Inhibitory interneurons are recruited to dampen hyperexcitability and prevent excitotoxicity to promote functional recovery (Carmichael et al., 2012; Medalla & Chang et al. 2020). Thus, we investigated the density of cfos$^+$ activated inhibitory neuron sub-types labeled for the calcium binding proteins, parvalbumin (PV), calbindin (CB), and calretinin (CR) in upper versus deep layers of dPMC (Fig. 3D, E, F). These inhibitory neuron

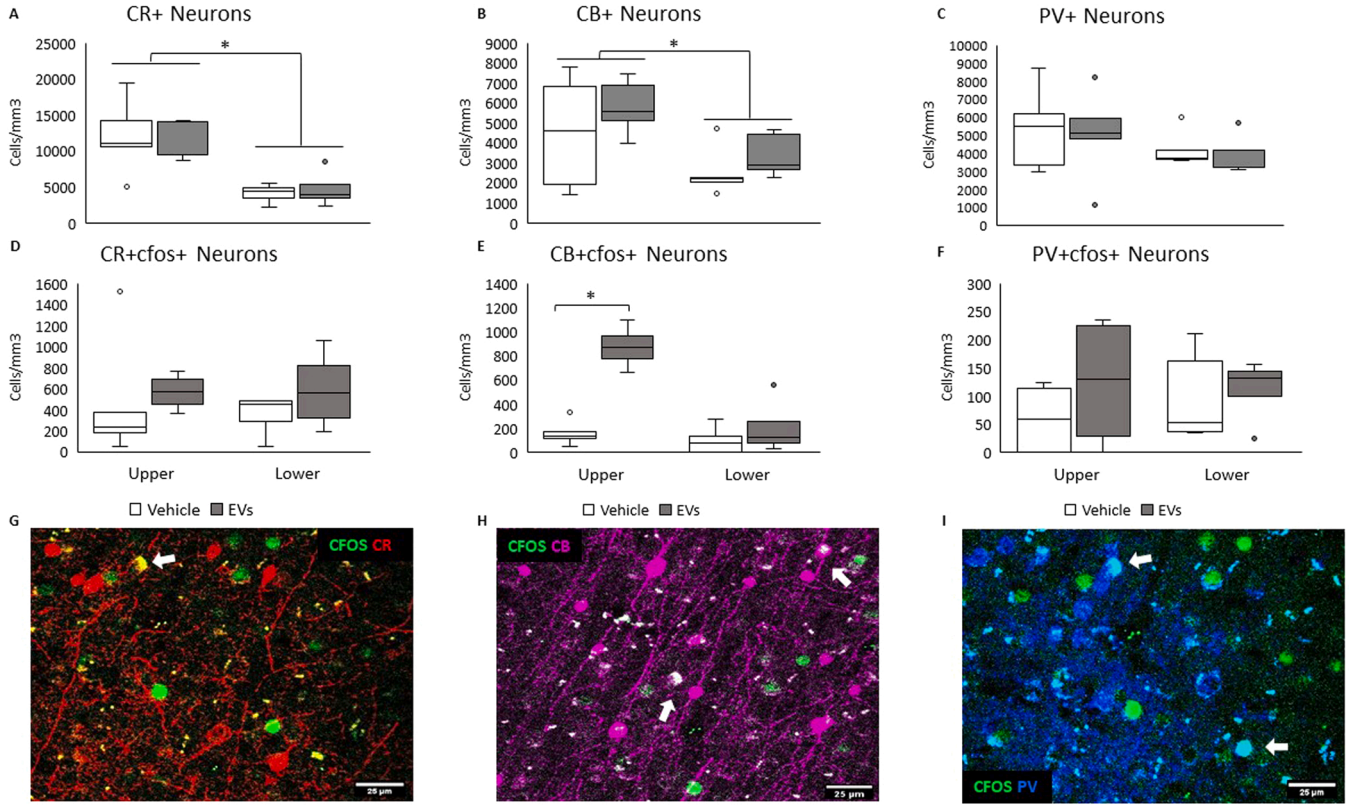

Fig. 3. MSCd-EV Effects on Task-relevant cfos$^+$ Activation of Inhibitory Interneurons in the dPMC: **A-C**) Box and whisker plots showing the density of single labeled inhibitory interneurons expressing the calcium binding proteins calretinin (CR), calbindin (CB), or parvalbumin (PV). **D-F)** Box and whisker plots showing the density of double labeled, presumably task-related, neurons with cfos and calcium binding proteins (CR, CB, PV). **G-I**) Representative confocal images of interneuron markers and cfos. Gray/White circles represent outliers on the graphs. Scale bars 25 μm.

subtypes constitute three non-overlapping populations that have distinct innervation patterns and modes of inhibition in the primate cortex (DeFelipe, 1997 review). Two-way ANOVAs showed that the density of CR, CB, and PV total cells did not significantly differ between groups (CR: $F(9,1)= 0.644$, $P = 0.438$; CB: $F(9,1)= 1.254$, $P = 0.285$; PV: $F(9,1)= 2.965$, $P = 0.111$; Fig. 3A-C). However, post-hoc Student T-tests with Bonferroni corrections show CR^+ ($P = 0.00004$; Fig. 3 A) and CB^+ ($P = 0.019$; Fig. 3B) neurons were denser in the upper (1−3) layers compared to deeper (4−6) layers, while PV^+ neurons had more equal distribution across all layers ($P = 0.310$; Fig. 3 C), which is consistent with previous literature (Condé et al., 1994).

The proportion of $cfos^+$ cells for each subtype was further evaluated. A two-way ANOVA of CR^+cfos^+ neurons (Fig. 3D) reveal no effect of group ($F(9,1)= 0.079$, $P = 0.784$), or layer ($F(9,1)= 0.007$, $P = 0.937$), and no interactions ($F(9,1)= 0.389$, $P = 0.545$). Similarly, two-way ANOVA of PV^+cfos^+ neurons (Fig. 3 F) shows no significant difference between groups ($F(9,1)= 1.523$, $P = 0.241$), no effect of layers ($F(9,1)= 0.278$, $P = 0.608$), and no significant interactions ($F(9,1)= 0.001$, $P = 0.994$). A two-way ANOVA of CB^+cfos^+ neurons (Fig. 3E) shows no difference between groups ($F(9,1)= 2.731$, $P = 0.124$), but a significant effect of layer ($F(9,1)= 21.651$, $P = 0.0005$) and significant interactions between group and layer ($F(9,1)= 7.238$, $P = 0.019$). Post-Hoc Student T-tests with Bonferroni corrections show treated monkeys have significantly more CB^+cfos^+ neurons in the upper layers ($P = 0.003$), but no treatment related differences in deep layers ($P = 0.864$). Consistent with our previous findings of the vPMC (Medalla & Chang et al. 2020), these data indicate an increased activity of the inhibitory CB^+ interneurons in the upper layers of the dPMC in treated monkeys.

MSCd EVs reduce LMN synapses in ventral horn LMNs

Since evidence suggests EV treatment prevented upper motor neuron loss and dysfunction in the periM1, we further investigated the reorganization of cortico-spinal projections at the level of the cervical spinal cord (CSC). We then assessed the density of putative synaptic connections in the ventral horn (VH) of the spinal cord during recovery

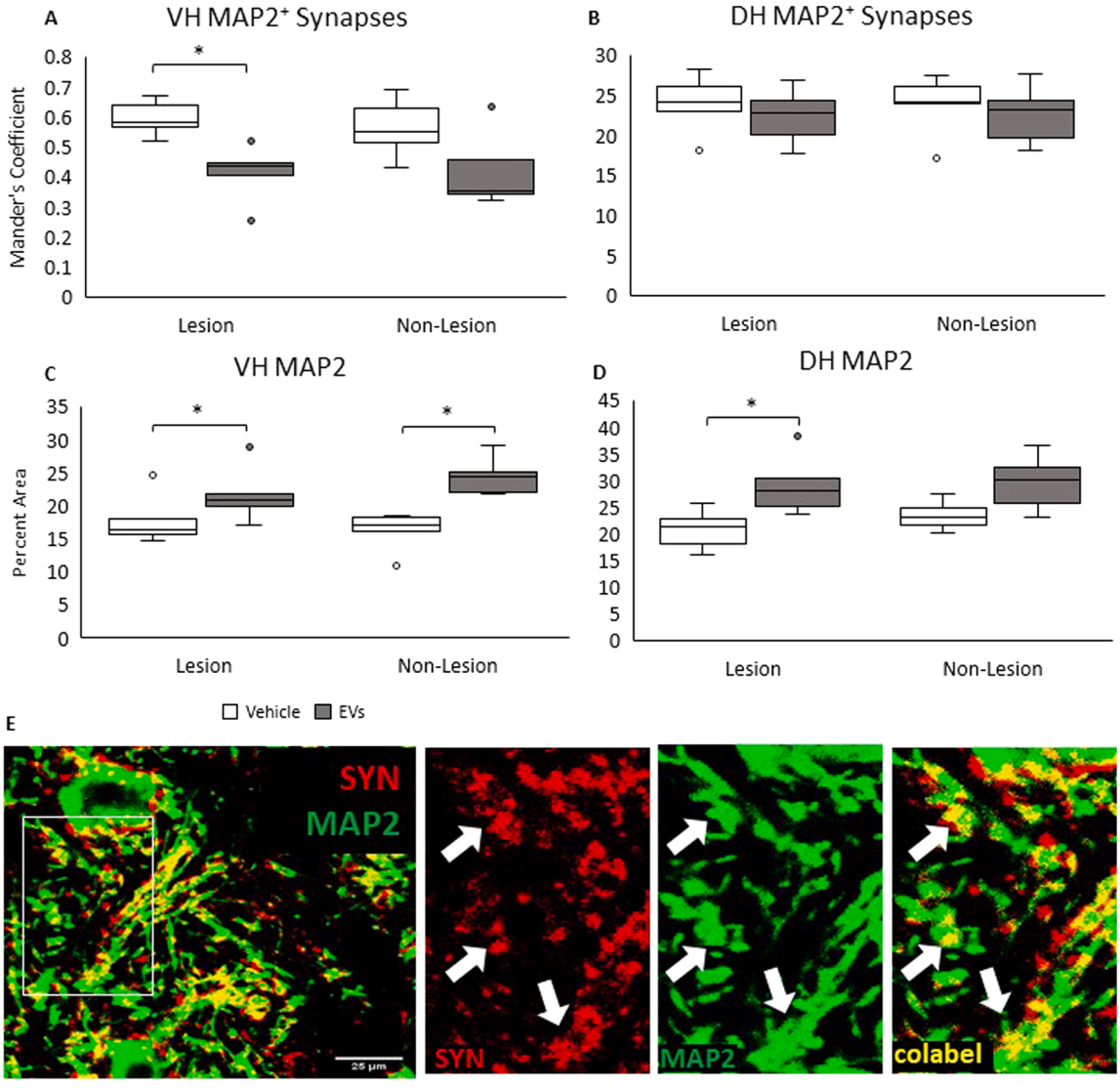

Fig. 4. MSCd-EV Effects on Axonal Sprouting, Synapse Density and Dendrite Density in Spinal Cord: (**A,B**) CLC of synaptic maker, SYN, with dendritic marker, MAP2, as an estimate of putative synapses in the contralesional (lesioned pathway) and ipsilesional (non-lesioned pathway) ventral horn (VH; A) as well as the dorsal horn (DH; B) in order to assess changes outside the motor circuit. (**C,D**) Percent area label of MAP2 expression in the contralesional (lesioned pathway) and ipsilesional (non-lesioned pathway) VH (C) and DH (D). E (**E**) Representative confocal image and inset in higher magnification, showing SYN^+ axon terminals in the red channel, $MAP2^+$ somas and dendrites in the green channel, and the SYN^+MAP2^+ colocalization in the merged channel, with colocalization in yellow (white arrows) in VH of the cervical spinal cord. Gray/White circles represent outliers on the graphs. Scale bars 25 μm.

(Fig. 4E) by quantifying the CLC of the presynaptic protein SYN, localized on synaptic active zones, and MAP2, a protein expressed by the LMN somas and dendrites. In the VH, where LMNs reside, a two-way ANOVA of $SYN^{+}MAP2^{+}$ CLC (Fig. 4 A) showed a significant difference between treatment groups ($F(9,1)= 11.164$, $P = 0.0049$), no significant effect of hemisphere ($F(9,1)= 0.264$, $P = 0.615$) and no interactions ($F(9,1)= 0.181$, $P = 0.676$). Post-hoc Student T-tests with Bonferroni corrections reveal that EV treated monkeys have significantly fewer $SYN^{+}MAP2^{+}$ putative synapses in the contralesional VH (lesioned pathway; $P = 0.019$) but no differences in the ipsilesional VH (non-lesioned pathway; $P = 0.183$).

To see if these UMN injury effects are specific to the VH, we also examined the dorsal horn (DH), where the sensory neurons of the CSC receive inputs from peripheral somatosensory receptors. In the DH (Fig. 4B) a two-way ANOVA showed no significant difference between hemispheres ($F(9,1)= 1.27$, $P = 0.292$) or groups ($F(9,1)= 0.855$, $P = 0.382$) and no interactions ($F(9,1)= 1.85$, $P = 0.211$). These data show that EV treated monkeys have significantly fewer $SYN^{+}MAP2^{+}$ putative synaptic interactions in the VH compared to vehicle controls.

MSCd EVs increase MAP2 staining in the ventral horn

Finally, dendritic complexity and MAP2 expression are reduced when LMNs are denervated (Jones and Thomas, 1962; Kolb and Winshaw, 1998). Hence, we evaluated density of dendritic MAP2 expression in the VH and DH of the CSC. A two-way ANOVA of MAP2 percent area labeled in the VH (Fig. 4 C) showed a significant difference between groups ($F(9,1)= 21.069$, $P = 0.0004$), no significant effect of hemispheres ($F(9,1)= 0.395$, $P = 0.538$), and no interactions ($F(9,1)= 0.398$, $P = 0.538$). Post-Hoc Student T-tests with Bonferroni corrections revealed that compared to vehicle, EV treated monkeys had significantly more MAP2 staining in the contralesional (lesioned pathway; $P = 0.044$) and ipsilesional VH (non-lesioned pathway; $P = 0.007$). Additionally, outside of the motor circuit a two-way ANOVA of MAP2% area in the DH (Fig. 4D) showed a significant difference between groups ($F(9,1)= 15.295$, $P = 0.0016$), no effect of hemispheres ($F(9,1)= 0.144$, $P = 0.710$) and no interactions ($F(9,1)= 0.112$, $P = 0.743$). Post-Hoc Student T-tests with Bonferroni corrections show increased MAP2 expression in the contralesional DH (lesioned pathway; $P = 0.049$) of EV versus vehicle treated monkeys, and no differences in the ipsilesional DH (non-lesioned pathway; $P = 0.13156$). In summary, we found total MAP2 staining in the EV treated monkeys was significantly greater in both the ipsilesional and contralesional VHs as well as in the contralesional DH, compared to those in vehicle treated monkeys.

Cortical and cervical spinal neuronal distribution and structure correlate with measures of recovery

Multiple linear correlation analysis showed an association between both cortical neuronal distribution and spinal cord structural outcomes with measures of faster motor recovery. The number of periM1 $SMI32^{+}cfos^{+}$ task-related neurons were negatively correlated with days to return to pre-op retrieval latencies ($R=0.579$, $P = 0.015$; Fig. 5 A) and trending with days to pre-op grasp patterns ($R=0.392$, $P = 0.058$; Fig. 5 A). In the dPMC upper layers, the presumably task-related $CB{+}cfos^{+}$ inhibitory interneuron exhibited a significant negative correlation with days to pre-op retrieval latencies ($R=0.679$, $P = 0.017$; Fig. 5B). In the VH, the contralesional $SYN^{+}MAP2^{+}$ CLC showed a positive trend with days to pre-op retrieval latencies ($R=0.626$, $P = 0.083$; Fig. 5 C). Lastly, contralesional MAP2 staining in the VH was

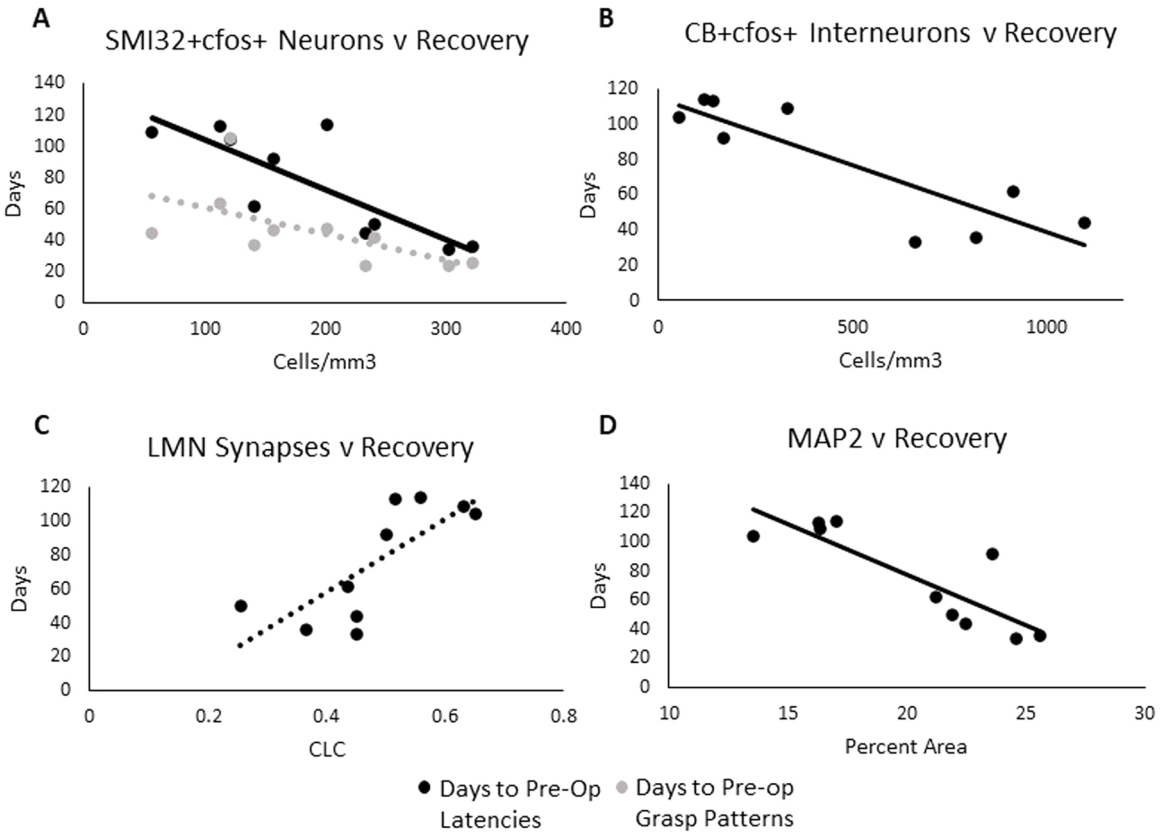

Fig. 5. Relationships with Motor Performance: Multiple linear correlations show significant correlations between histological measures and motor recovery measured as the number of days it took animals to return to pre-op functions. **A**) Task activated pyramidal neurons (SMI32+cfos+) in the periM1 and **B**) task activated calbindin interneurons (CB+cfos+) in the dPMC are associated with recovery of pre-op functions. Additionally, in the contralesional VH **C**) fewer LMN synapses and **D**) great MAP2+ expression associated with faster recovery of retrieval latencies.

negatively correlated with days to pre-op retrieval latencies (R=0.769, P = 0.026; Fig. 5D). In summary these data show that increasing cfos$^+$ activity of pyramidal neurons in the periM1 as well as the activity of inhibitory interneurons in the upper dPMC correlated with faster recovery of motor function. Additionally, fewer SYN$^+$MAP2$^+$ synapses in the VH and increased MAP2 staining also correlated with improved functional recovery.

Discussion

In this study, we investigated the efficacy of MSCd EVs to reduce the cascade of secondary damage that follows cortical injury and how it contributes to neuronal recovery of the cortical and spinal motor circuits. Our previous study reported that monkeys treated with EVs evidence a significant recovery of fine motor function of the hand during the first few weeks after cortical injury in M1 and attain a full return to pre-operative retrieval latencies and grasp patterns by 14 weeks post-injury (Moore et al., 2019). In the present study, histological examination 14 weeks after injury revealed that EV treatment was associated with 1) greater densities of SMI32$^+$ pyramidal neurons in deep layers 5–6 of periM1, including the subset double-labeled with cfos$^+$ and 2) in the dPMC, greater densities of presumably task-related cfos$^+$ inhibitory interneurons in the upper layers, compared with vehicle treatment. In the CSC, EV group exhibited 1) lower LMN synaptic density in the contralesional VH with 2) a bilateral increase in dendritic MAP2 expression. These treatment-related differences in upper and lower motor neurons were associated with improved functional outcomes.

Cortical remodeling

In this study, we showed that increased task-related cfos activation of SMI32$^+$ pyramidal neurons in periM1 were significantly correlated with improved functional recovery of treated monkeys. Specifically, deep layer 5–6 pyramidal neurons in PMC and M1 contribute to cortico-spinal projections (Ralston et al., 1985; Dum and Strick, 1991, Hof et al., 1995; Morecraft et al., 2013, 2019) and are enriched with SMI32, a non-phosphorylated neurofilament heavy chain protein (Tsang et al., 2000). In the current study, EV treated monkeys had a greater density of intact and task-related SMI32$^+$ pyramidal neurons in periM1 deep layers. This suggests that after injury, EV-treated monkeys may have had less secondary damage to M1 promoting survival and function of UMNs, particularly those that send long distance projections to the spinal cord.

Our previous studies have shown that increased cfos activation in the vPMC following injury in M1 is correlated with functional recovery (Orczykowski et al., 2018; Medalla & Chang, 2021). In the current study, we specifically showed a strong correlation between recovery and increased cfos activity of inhibitory interneurons in upper cortical layers of dPMC. Hyperexcitability is a common consequence of cortical injury (Carmichael, 2012; Kohman and Rhodes, 2013; Lai et al., 2014; Jayaraj et al., 2019) due to increased extracellular glutamate concentration and stimulation of the neuronal death cascade (Lai et al., 2014). Inflammatory astrocytes and microglia have been shown to further promote excitotoxicity (Vinet et al., 2012; Pekny et al., 2016). However, MSCd EVs can modulate inflammatory responses in rodent models (Di Trapani et al., 2016; Phinney et al., 2017; Zhang et al., 2014), including reduction of astrogliosis (Xian et al., 2019) and microglia reactivity (Ruppert et al., 2018; Howe and Barres, 2012). We previously reported in monkeys that MSCd EVs encourage ramified microglia after cortical injury (Go et al., 2020) and using single-cell in vitro electrophysiology of vPMC pyramidal neurons, we showed that EV treatment promoted restoration of E:I balance (Medalla & Chang et al., 2020). We expand on this work by showing inhibitory task-related cfos+ activity in the dPMC was also associated with laminar specific pyramidal neuron activity in periM1. Greater cfos activation of CB$^+$ inhibitory neurons with EV treatment suggests a mechanism by which increased inhibitory inputs onto pyramidal neurons may help maintain the excitatory and inhibitory balance and is consistent with our previous electrophysiology (Medalla & Chang et al., 2019). CB$^+$ neurons, which target distal dendrites of pyramidal neurons to modulate dendritic excitability, are highly resistant to hyperexcitability after injury (Mattson et al., 1991; Phillips et al., 1999; D'Orlando et al., 2002) and may play an important role in recovery after injury. Although further investigation of molecular effects on inhibitory mechanisms is needed, the combination of greater number of intact pyramidal neurons in the deep layers of periM1 and potential balancing of excitatory and inhibitory activity in PMC with EV treatment may allow greater control of LMNs and motor function.

Spinal cord plasticity

After injury to the motor cortex, upper motor neurons die leading to reduced signals to LMNs (Lipton, 1999). During recovery, plasticity in the cortex can occur to reorganize motor circuits (Carmichael et al., 2003; Nudo, 2006; Dancause et al., 2005; Kantak et al., 2012). Yet, even for UMNs that survive the lesion, their long-distance cortico-spinal projections into the lateral corticospinal tract (LCST) could be susceptible to damage and therefore limit the recovery of fine motor movements. However, plasticity in the LCST axon terminations and LMNs within the spinal cord may compensate for loss of cortical input. Indeed, studies have shown, in both rodents and primates, intact CST axons send collaterals and increase synaptic connections with denervated neurons after injury (Wiessner et al., 2003; Weidner et al., 2001; Lee et al., 2004; Zai et al., 2009; Wahl et al., 2014; Fouad et al., 2004; Freund et al., 2006; Rosenzweig et al. 2009, 2010). However, it has also been noted that aberrant plasticity after nerve injury can be harmful to functional recovery (Kim et al., 2015; Beauparlant et al., 2013). Specifically, in rodents, Kim et al. (2015) showed a negative correlation between cortical synaptic density and functional improvement after stroke, and Beauparlant et al. (2013) reveals increased synaptic plasticity after axonal injuries correlated with motor neuron dysfunction. As follows, our study shows EV treated monkeys have significantly fewer VH synapses compared to vehicle-treated control monkeys. Additionally, increased VH synapses correlated with worse behavioral outcomes suggesting too many aberrant connections could interfere with motor recovery. EV treatment may have reduced undirected aberrant plasticity either by preserving LMN innervations due to reduced cortical damage, as evidenced by a greater number of intact and task-activated M1 pyramidal neurons, or acted independently in the spinal cord to direct LMN plasticity in a more specified manner. Moreover, MAP2 expression is increased in the CSC of EV treated monkeys, which is consistent with our previous data showing increased dendritic branching complexity in cortical pyramidal neurons (Medalla & Chang et al., 2020). MAP2 is required for dendritic growth and stabilization (Harada et al., 2002) and studies have shown that when neurons lose their afferent connections, dendrites begin to atrophy (Jones and Thomas, 1962; Kolb and Winshaw, 1998). Therefore, maintenance of upper motor neuron connections may have prevented dendritic atrophy of LMNs in EV-treated monkeys. Further investigation is needed to determine the mechanism and specific effects of EVs on spinal cord circuits.

Bilateral effects of EV treatment on CSC MAP2 expression may suggest contributions of UMN pathways from both contralesional (lesioned) and ipsilesional (non-lesioned) motor areas, of which both pathways have been shown to play a role in spinal cord reorganization after cortical injury (Buetefisch, 2015; Zai et al., 2009; Gonzalez et al., 2004; Hoff and Hoff, 1934; Tigges et al., 1979; Nakagawa, 1980; Ralston & Ralston, 1985; Alawieh et al., 2017). Interestingly, we also saw significant differences of MAP2 staining between EV and vehicle treated monkeys in the contralesional somatosensory neurons of the DH as well. These data suggest that EVs may have a more global effect on spinal cord dendrites or that injury to the motor cortex may have induced changes in the complementary sensory regions. Indeed, studies indicate that motor learning affects both motor and sensory areas of the brain (Ostry et al., 2010, 2016) and recovery after stroke can recruit activity from sensory

and motor areas (Zemke et al., 2003). Further investigation is needed to understand these recovery- and treatment-related changes in dendritic structure in distinct sensory and motor cortical and spinal cord regions.

Conclusion

The consequences of cortical injury can lead to long lasting disability and loss of fine motor function. Although there are treatments to remove vessel blockages to re-perfuse tissue (Koroshetz, 1996), there are currently no FDA approved treatments to improve neural recovery after injury. EVs derived from mesenchymal stem cells are filled with immune modulating and growth signaling miRNA, mRNA, and proteins (Chopp et al., 2009; Di Trapanni et al., 2016; Casado et al., 2017), which may be beneficial for neural repair. While future molecular and proteomic studies are underway to assess the specific content of these MSC-EVs derived from monkey bone marrow, our series of studies show that EV treatment after cortical injury improves functional fine motor recovery (Moore et al., 2019), decreases perilesional inflammatory microglia and myelin damage (Go et al., 2020, 2021), reduces hyperexcitability, and maintains E:I balance in vPMC neurons (Medalla & Chang et al., 2020). In the current study we showed that EV treatment is further associated with reorganization of cortical and spinal motor circuits. Specifically in the cortex, EVs appear to promote pyramidal neuron survival and task-related $cfos^{+}$ activation in L5/6 of periM1 and inhibitory interneuron activity in the dPMC. In the spinal cord, EVs reduced potential aberrant synaptic plasticity in the VH as evidenced by fewer $SYN^{+}MAP2^{+}$ synapses. Hence, the immune and growth signals from MSCd EVs may contribute to the observed faster recovery of motor function after cortical injury by reducing neuronal damage and denervation of LMNs as well as dampening dysfunctional plasticity. Overall, our data demonstrate that MSCd EVs are a potential therapeutic for increasing functional recovery after cortical injury, likely through multifaceted mechanisms of inflammation and neural plasticity.

Funding

This work was supported by the National Institutes of Health [NIH/NINDS R56 NS112207, NIH/NIA R21 NS111174, NIH/NINDS R21-NS102991].

Acknowledgments

Payton E Cabrera for executing immunofluorescence staining of spinal cord.

References

Alawieh A., Tomlinson S., Adkins D., Kautz S., Feng W.. Preclinical and Clinical Evidence on Ipsilateral Corticospinal Projections: Implication for Motor Recovery. Transl Stroke Res. 2017 Dec;8(6):529–540. doi: 10.1007/s12975–017-0551–5. Epub 2017 Jul 9. PMID: 28691140; PMCID: PMC5802360.

Aleynik, A., Gernavage, K.M., Mourad, Y.S.H., Sherman, L.S., Liu, K., Gubenko, Y.A., Rameshwar, P., 2014. Stem cell delivery of therapies for brain disorders. Clin. Transl. Med 3, 24. https://doi.org/10.1186/2001-1326-3-24.

Banks, W.A., Sharma, P., Bullock, K.M., Hansen, K.M., Ludwig, N., Whiteside, T.L., 2020. Transport of Extracellular Vesicles across the Blood-Brain Barrier: Brain Pharmacokinetics and Effects of Inflammation. Int J. Mol. Sci. 21 (12), 4407. https://doi.org/10.3390/ijms21124407.

Barbas, H., Pandya, D.N., 1987. Architecture and frontal cortical connections of the premotor cortex (area 6) in the rhesus monkey. J. Comp. Neurol. 256, 211–228. https://doi.org/10.1002/cne.902560203.

Barros, V.N., Mundim, M. Galindo, L.T., Bittencourt, S., Porcionatto, M., and Mello L.E. "The pattern of cfos expression and its refractory period in the brain of rats and monkeys" Front. Cell. Neurosci. 2015 | https://doi.org/10.3389/fncel.2015.00072.

Benjamin E.J., Blaha M.J., Chiuve S.E., et al. "On behalf of the American Heart Association Statistics Committee and Stroke Statistics Subcommittee. Heart disease and stroke statistics—2017 update: a report from the American Heart Association." Circulation. 2017; 135:e229-e445.

Beauparlant, J., van den Brand, R., Barraud, Q., Friedli, L., Musienko, P., Dietz, V., Courtine, G., 2013. Undirected compensatory plasticity contributes to neuronal dysfunction after severe spinal cord injury. Brain 136 (11), 3347–3361. https://doi.org/10.1093/brain/awt204.

Buetefisch, C.M., 2015. Role of the contralesional hemisphere in post-stroke recovery of upper extremity motor function (eCollection). Front Neurol. 2015 Oct. 16 6, 214. https://doi.org/10.3389/fneur.2015.00214.

Campbell MJ1, Morrison, J.H., 1989. Monoclonal antibody to neurofilament protein (SMI-32) labels a subpopulation of pyramidal neurons in the human and monkey neocortex. J. Comp. Neurol. 282 (2), 191–205. Apr 8.

Carmichael, S.T., 2003. Plasticity of cortical projections after stroke. Neuroscientist 9 (1), 64–75. https://doi.org/10.1177/1073858402239592.

Carmichael, S.T., 2006. Cellular and molecular mechanisms of neural repair after stroke: making waves. An. Neurol. 59 (5), 735–742. https://doi.org/10.1002/ana.20845.

Carmichael, S.T., 2012. Brain excitability in stroke: the yin and yang of stroke progression. Arch. Neurol. 69, 161–167.

Casado, J.G., Blazquez, R., Vela, F.J., Alvarez, V., Tarazona, R., Sanchez-Margallo, F.M., 2017. Mesenchymal stem cell-derived exosomes: immunomodulatory evaluation in an antigen-induced synovitis porcine model. Front Vet. Sci. 4, 39. https://doi.org/10.3389/fvets.2017.00039.

Chopp, M., Li, Y., amp; Zhang, Z.G., 2009. Mechanisms underlying improved recovery of neurological function after stroke in the rodent after treatment with neurorestorative cell-based therapies. Stroke 40 (3 Suppl), S143–S145. https://doi.org/10.1161/STROKEAHA.108.533141.

Condé, F., Lund, J.S., Jacobowitz, D.M., Baimbridge, K.G., Lewis, D.A., 1994. Local circuit neurons immunoreactive for calretinin, calbindin D-28k or parvalbumin in monkey prefronatal cortex: Distribution and morphology. J. Comp. Neurol. 341 (1), 95–116. https://doi.org/10.1002/cne.903410109.

Cuartero, M.I., de la Parra, J., Pérez-Ruiz, A., Bravo-Ferrer, I., Durán-Laforet, V., García-Culebras, A., Manuel García-Segura, J., Dhaliwal, J., Frankland, P.W., Lizasoain, I., Ángeles Moro, M., 2019. Abolition of aberrant neurogenesis ameliorates cognitive impairment after stroke in mice. J. Clin. Invest 129 (4), 1536–1550. https://doi.org/10.1172/JCI120412.

Dancause N1, Barbay, S., Frost, S.B., Plautz, E.J., Chen, D., Zoubina, E.V., Stowe, A.M., Nudo, R.J., 2005. Extensive cortical rewiring after brain injury. J. Neurosci. 25 (44). Nov 2.

Darling W.G., Pizzimenti M.A., Morecraft R.J. Functional recovery following motor cortex lesions in non-human primates: experimental implications for human stroke patients. J Integr Neurosci. 2011 Sep;10(3):353–84. doi: 10.1142/S0219635211002737. PMID: 21960307; PMCID: PMC3689229.

Di Trapani, M., Bassi, G., Midolo, M., Gatti, A., Kamga, P.T., Cassaro, A., Carusone, R., Adamo, A., Krampera, M., 2016. "Differential and transferable modulatory effects of mesenchymal stromal cell-derived extracellular vesicles on T, B and NK cell functions.". Sci. Rep. 6, 24120. https://doi.org/10.1038/srep24120.

(D') Orlando, C., Celio, M.R., Schwaller, B., 2002. Calretinin and calbindin D-28k, but not parvalbumin protect against glutamate-induced delayed excitotoxicity in transfected N18-RE 105 neuroblastoma-retina hybrid cells, Aug 2 Brain Res 945 (2), 181–190. https://doi.org/10.1016/s0006-8993(02)02753-1.

Dum, R.P., Strick, P.L., 1991. The origin of corticospinal projections from the premotor areas in the frontal lobe. J. Neurosci. 11 (3), 667–689. https://doi.org/10.1523/JNEUROSCI.11-03-00667.1991.

Fouad, K., Klusman, I., Schwab, M.E., 2004. Regenerating corticospinal fibers in the Marmoset (Callitrix jacchus) after spinal cord lesion and treatment with the anti-Nogo-A antibody IN-1. Eur. J. Neurosci. 20 (9) (Nov).

Freund, P., Schmidlin, E., Wannier, T., Bloch, J., Mir, A., Schwab, M.E., Rouiller, E.M., 2006. Nogo-A-specific antibody treatment enhances sprouting and functional recovery after cervical lesion in adult primates. Nat. Med 12 (7), 790–792 (Jul).

Gennaro, M., Mattiello, A., Mazziotti, R., Antonelli, C., Gherardini, L., Guzzetta, A., Berardi, N., Cioni, G., Pizzorusso, T., 2017. Focal stroke in the developing rat motor cortex induces age- and experience-dependent maladaptive plasticity of corticospinal system. Front. Neural Circuits 11 (47). https://doi.org/10.3389/fncir.2017.00047.

Go, V., Bowley, B.G.E., Pessina, M.A., Zhang, Z.G., Chopp, M., Finkelstein, S.P., Rosene, D.L., Medalla, M., Buller, B., Moore, T.L., 2020. Extracellular vesicles from mesenchymal stem cells reduce microglial-mediated neuroinflammation after cortical injury in aged Rhesus monkeys. GeroScience 42 (1), 1–17. https://doi.org/10.1007/s11357-019-00115-w.

Go, V., Sarikaya, D., Zhou, Y., Bowley, B.G.E., Pessina, M.A., Rosene, D.L., Zhang, Z.G., Chopp, M., Finklestein, S.P., Medalla, M., Buller, B., Moore, T.L., 2021. Extracellular vesicles derived from bone marrow mesenchymal stem cells enhance myelin maintenance after cortical injury in aged rhesus monkeys. Exp. Neurol. 337, 113540 https://doi.org/10.1016/j.expneurol.2020.113540.

Gonzalez, C.L., Gharbawie, O.A., Williams, P.T., Kleim, J.A., Kolb, B., Whishaw, I.Q., 2004. Evidence for bilateral control of skilled movements: ipsilateral skilled forelimb reaching deficits and functional recovery in rats follow motor cortex and lateral frontal cortex lesions. Eur. J. Neurosci. 20 (12), 3442-52.

Grefkes, C., Ward, N.S., 2014. Cortical reorganization after stroke: how much and how functional? (Feb). Neuroscientist 20 (1), 56–70. https://doi.org/10.1177/1073858413491147.

Guzowski, J.F., McNaughton, B.L., Barnes, C.A., Worley, P.F., 1999. Environment-specific expression of the immediate-early gene Arc in hippocampal neuronal ensembles. Nat. Neurosci. 2, 1120–1124. https://doi.org/10.1038/16046.

Hall, J., Thomas, K.L., Everitt, B.J., 2001. Cellular imaging of zif268 expression in the hippocampus and amygdala during contextual and cued fear memory retrieval: selective activation of hippocampal CA1 neurons during the recall of contextual memories. J. Neurosci. 21, 2186–2193.

Harada, A., Teng, J., Takei, Y., Oguchi, K., Hirokawa, N., 2002. MAP2 is required for dendrite elongation, PKA anchoring in dendrites, and proper PKA signal transduction. J. Cell Biol. 158 (3), 541–549. https://doi.org/10.1083/jcb.200110134.

Hoff, E., Hoff, H., 1934. Spinal terminations of the projection fibers from the motor cortex of primates. Brain.
Hof, P.R., Nimchinsky, E.A., Morrison, J.H., 1995. Neurochemical phenotype of corticocortical connections in the macaque monkey: quantitative analysis of a subset of neurofilament protein-immunoreactive projection neurons in frontal, parietal, temporal, and cingulate cortices. J. Comp. Neurol. 362 (1), 109–133.
Howe, M.L., Barres, B.A., 2012. A novel role for microglia in minimizing excitotoxicity. Jan 31 BMC Biol. 10, 7. https://doi.org/10.1186/1741-7007-10-7.
Jayaraj, R.L., Azimullah, S., Beiram, R., Jalal, F.Y., Rosenberg, G.A., 2019. Neuroinflammation: friend and foe for ischemic stroke. J. Neuroinflamm. 16, 142.
Johansen-Berg, H., Rushworth, M.F., Bogdanovic, M.D., Kischka, U., Wimalaratna, S., Matthews, P.M., 2002. The role of ipsilateral premotor cortex in hand movement after stroke. Proc. Natl. Acad. Sci. USA 99, 14518–14523. https://doi.org/10.1073/pnas.222536799.
Jones, W.H., Thomas, D.B., 1962. Changes in the dendritic organization of neurons in the cerebral cortex following deafferentation. J. Anat. 96, 375–381.
Kantak, S.S., Stinear, J.W., Buch, E.R., Cohen, L.G., 2012. Rewiring the brain: potential role of the premotor cortex in motor control, learning, and recovery of function following brain injury. Neurorehabil Neural Repair 26, 282–292. https://doi.org/10.1177/1545968311420845.
Katakowski, M., Buller, B., Zheng, X., Lu, Y., Rogers, T., Osobamiro, O., Chopp, M., 2013. Extracellular vesicles from marrow stromal cells expressing miR-146b inhibit glioma growth. Cancer Lett. 335 (1), 201–204. https://doi.org/10.1016/j.canlet.2013.02.019.
Kim, S.Y., Allred, R.P., Adkins, D.L., Tennant, K.A., Donlan, N.A., Kleim, J.A., Jones, T.A., 2015. Experience with the "good" limb induces aberrant synaptic plasticity in the perilesion cortex after stroke. J. Neurosci. 35 (22), 8604–8610. https://doi.org/10.1523/JNEUROSCI.0829-15.2015.
Kohman, R.A., Rhodes, J.S., 2013. Neurogenesis, inflammation and behavior. Brain Behav. Immun. 27, 22–32.
Kolb, B., Winshaw, I.Q., 1998. Brain plasticity and behavior. Annu. Rev. Psychol. 49, 43–64. https://doi.org/10.1146/annurev.psych.49.1.43.
Koroshetz WJ1, Moskowitz M.A.C., 1996. Emerging treatments for stroke in humans. Trends Pharm. Sci. 17 (6), 227-33.
Kwakkel, G., Winters, C., van Wegen, E.E., Nijland, R.H., van Kuijk, A.A., Visser-Meily, A., Consortium, E.-S., 2016. Effects of unilateral upper limb training in two distinct prognostic groups early after stroke: the EXPLICIT-stroke randomized clinical trial, 804-16 Neurorehabil Neural Repair 30 (9). https://doi.org/10.1177/1545968315624784.
Lai, T.W., Zhang, S., Wang, Y.T., 2014. Excitotoxicity and stroke: identifying novel targets for neuroprotection. Prog. Neurobiol. 115, 157–188.
Lakhan, S.E., Kirchgessner, A., amp; Hofer, M., 2009. Inflammatory mechanisms in ischemic stroke: therapeutic approaches. J. Transl. Med 7, 97. https://doi.org/10.1186/1479-5876-7-97.
Lambertsen, K.L., Finsen, B., Clausen, B.H. "Post-stroke inflammation- target or tool for therapy"? Acta Neuropathol. 2018. Epub ahead of print. doi:10.1007/s00401–018-1930-z.
Lee, J.K.1, Kim, J.E., Sivula, M., Strittmatter, S.M., 2004. Nogo receptor antagonism promotes stroke recovery by enhancing axonal plasticity. J. Neurosci. 24 (27), 6209-17.
Lee, T.K., Hong, J., Lee, J.W., Kim, S.S., Sim, H., Lee, J.C., Kim, D.W., Lim, S.S., Kang, J., Won, M.H., 2021. Ischemia-induced cognitive impairment is improved via remyelination and restoration of synaptic density in the hippocampus after treatment with COG-Up® in a gerbil model of ischemic stroke. Vet. Sci. 8 (12), 321. https://doi.org/10.3390/vetsci8120321.
Leon-Jimenez, J.L., Ruiz-Sandoval Chiquete, E., et al., 2014. Hospital arrival time and functional outcome after acute ischaemic stroke: results from the PREMIER study. Neurologia 29, 200–209.
Link, W., Konietzko, U., Kauselmann, G., Krug, M., Schwanke, B., Frey, U., et al. "Somatodendritic expression of an immediate early gene is regulated by synaptic activity." Proc. Natl. Acad. Sci. U.S.A. 1995; 92:5734–5738. doi: 10.1073/pnas.92.12.5734.
Lipton, P.Ischemic cell death in brain neurons. Physiol Rev. 1999; 79(4):1431- 1568. doi: 10.1152/physrev.1999.79.4.1431.
Liu, Z., Li, Y., Zhang, Z.G., Cui, X., Cui, Y., Lu, M., Chopp, M., 2010. Bone marrow stromal cells enhance inter- and intracortical axonal connections after ischemic stroke in adult rats. J. Cereb. Blood Flow. Metab. 30 (7), 1288–1295. https://doi.org/10.1038/jcbfm.2010.8.
Lyford, G.L., Yamagata, K., Kaufmann, W.E., Barnes, C.A., Sanders, L.K., Copeland, N.G., et al., 1995. Arc, a growth factor and activity-regulated gene, encodes a novel cytoskeleton-associated protein that is enriched in neuronal dendrites. Neuron 14, 433–445. https://doi.org/10.1016/0896-6273(95)90299-6.
Mahmood, A., Lu, D., Qu, C., Goussev, A., Chopp, M., 2005. Human marrow stromal cell treatment provides long-lasting benefit after traumatic brain injury in rats. Neurosurgery 57 (5), 1026–1031 discussion 1026-1031.
Marei, H.E., Hasan, A., Rizzi, R., Althani, A., Afifi, N., Cenciarelli, C., Caceci, T., Shuaib, A., 2018. Potential of Stem Cell-Based Therapy for Ischemic Stroke. Front. Neurol. 9, 34. https://doi.org/10.3389/fneur.2018.00034.
Matsumoto, J., Stewart, T., Banks, W.A., and Zhang, J. "The Transport Mechanism of Extracellular Vesicles at the Blood-Brain Barrier" Current Pharm Design. 2017; 23 (40):6206–6214(9). https://doi.org/10.2174/1381612823666170913164738.
Mattson, M.P., Rychlik, B., Chu, C., Christakos, S., 1991. Evidence for calcium-reducing and excito-protective roles for the calcium-binding protein calbindin-D28k in cultured hippocampal neurons. Neuron 6 (1), 41–51. https://doi.org/10.1016/0896-6273(91)90120-o.
Maxwell, N., Castro, R.W., Sutherland, N.M., Vaughan, K.L., Szarowicz, M.D., de Cabo, R., Mattison, J.A., Valdez, G., 2018. α-Motor neurons are spared from aging while their synaptic inputs degenerate in monkeys and mice. Aging Cell 17 (2), e12726. https://doi.org/10.1111/acel.12726.
Medalla, M., Chang, W., Calderazzo, S.M., Go, V., Tsolias, A., Goodliffe, J.W., Pathak, D., De Alba, D., Pessina, M.A., Rosene, D.L., Buller, B., Moore, T.L., 2020. Treatment with mesenchymal-derived extracellular vesicles reduces injury-related pathology in pyramidal neurons of monkey perilesional ventral premotor cortex EVs reduce injury-related pathology in vPMC, 2226-19 J. Neuro. https://doi.org/10.1523/JNEUROSCI.2226-19.2020.
Morecraft, R.J., Ge, J., Stilwell-Morecraft, K.S., McNeal, D.W., Pizzimenti, M.A., Darling, W.G., 2013. Terminal distribution of the corticospinal projection from the hand/arm region of the primary motor cortex to the cervical enlargement in rhesus monkey. J. Comp. Neurol. 521 (18), 4205-35.
Morecraft, R.J., Ge, J., Stilwell-Morecraft, K.S., Rotella, D.L., Pizzimenti, M.A., Darling, W.G., 2019. Terminal organization of the corticospinal projection from the lateral premotor cortex to the cervical enlargement (C5-T1) in rhesus monkey. J. Comp. Neurol. 527, 2761–2789. https://doi.org/10.1002/cne.24706.
Morgan, J.I., Cohen, D.R., Hempstead, J.L., Curran, T., 1987. Mapping patterns of expression in the central nervous system after seizure. Science 237, 192–197. https://doi.org/10.1126/science.3037702.
Moore, T.L., et al., 2019. Mesenchymal derived exosomes enhance recovery of motor function in a monkey model of cortical. Injury' 347–362.
Moore, T.L., Killiany, R.J., Pessina, M.A., Moss, M.B., Rosene, D.L., 2010. Assessment of motor function of the hand in aged rhesus monkeys. Somat. Mot. Res 27 (3), 121–130. https://doi.org/10.3109/08990220.2010.485963.
Moore, T.L., Pessina, M.A., Finklestein, S.P., Killiany, R.J., Bowley, B., Benowitz, L., Rosene, D.L., 2016. Inosine enhances recovery of grasp following cortical injury to the primary motor cortex of the rhesus monkey. Restor. Neurol. Neurosci. 34 (5), 827–848. https://doi.org/10.3233/RNN-160661.
Nakagawa, S., 1980 9. Onuf's nucleus of the sacral cord in a South American monkey (Saimiri): its location and bilateral cortical input from area 4. Brain Res. 191 (2), 337-44.
Nishimura Y., Isa T. Cortical and subcortical compensatory mechanisms after spinal cord injury in monkeys. Exp Neurol. 2012 May;235(1):152–61. doi: 10.1016/j.expneurol.2011.08.013. Epub 2011 Aug 23. PMID: 21884698.
Niv, F., Keiner, S., Krishna, K., Witte, O.W., Chichung Lie, D., Redecker, C., 2012. Aberrant neurogenesis after stroke: a retroviral cell labeling study. Stroke 43, 2468–2475. https://doi.org/10.1161/STROKEAHA.112.660977.
Nudo, R.J., 2006. Mechanisms for recovery of motor function following cortical damage. Curr. Opin. Neurobiol. 16, 638–644.
Orczykowski, M.E., Arndt, K.R., Palitz, L.E., Kramer, B.C., Pessina, M.A., Oblak, A.L., Moore, T.L., 2018. Cell based therapy enhances activation of ventral premotor cortex to improve recovery following primary motor cortex injury. Exp. Neurol. 305, 13–25. https://doi.org/10.1016/j.expneurol.2018.03.010.
Ostry, D.J., Darainy, M., Mattar, A.A.G., Wong, J., Gribble, P.L., 2010. Somatosensory plasticity and motor learning. J. Neurosci. 30 (15), 5384–5393. https://doi.org/10.1523/JNEUROSCI.4571-09.2010.
Ostry, D.J., Gribble, P.L., 2016. Trends Neurosci. 39 (2), 114–123. Epub 2016 Jan 13.
Pekny M., Pekna M., Messing A., Steinhäuser C., Lee J.M., Parpura V., Hol E.M., Sofroniew M.V., Verkhratsky A. Astrocytes: a central element in neurological diseases. Acta Neuropathol. 2016 Mar;131(3):323–45. doi: 10.1007/s00401–015-1513–1. Epub 2015 Dec 15. PMID: 26671410.
Pessina, M.A., Bowley, B.G.E., Rosene, D.L., and Moore, T.L. "A method for assessing recovery of fine motor function of the hand in a rhesus monkey model of cortical injury: an adaptation of the Fugl–Meyer Scale and Eshkol–Wachman Movement Notation" Somatosensory & Motor Research. 2019; 36(1):69–77. https://doi.org/10.1080/08990220.2019.1594751.
Phillips, R.G., Meier, T.J., Giuli, L.C., McLaughlin, J.R., Ho, D.Y., Spolsky, R.M., 1999. Calbindin D28K gene transfer via herpes simplex virus amplicon vector decreases hippocampal damage in vivo following neurotoxic insults. JNC 73 (3), 1200–1205.
Phinney, D.G., Pittenger, M.F., 2017. Concise review: MSC-derived extracellular vesicles for cell-free therapy. Stem Cells 35 (4), 851–858. https://doi.org/10.1002/stem.2575.
Ralston, D.D., Ralston 3rd, H.J., 1985. The terminations of corticospinal tract axons in the macaque monkey. J. Comp. Neurol. 242 (3). Dec 15.
Ramirez-Amaya, V., Vazdarjanova, A., Mikhael, D., Rosi, S., Worley, P.F., Barnes, C.A., 2005. Spatial exploration-induced Arc mRNA and protein expression: evidence for selective, network-specific reactivation. J. Neurosci. 25, 1761–1768. https://doi.org/10.1523/JNEUROSCI.4342-04.2005.
Rosenzweig, E.S., Brock, J.H., Culbertson, M.D., Lu, P., Moseanko, R., Edgerton, V.R., Havton, L.A., Tuszynski, M.H., 2009. Extensive spinal decussation and bilateral termination of cervical corticospinal projections in rhesus monkeys. J. Comp. Neurol. 513 (2), 151–163. https://doi.org/10.1002/cne.21940.
Rosenzweig, E.S., Courtine, G., Jindrich, D.L., Brock, J.H., Ferguson, A.R., Strand, S.C., Nout, Y.S., Roy, R.R., Miller, D.M., Beattie, M.S., Havton, L.A., Bresnahan, J.C., Edgerton, V.R., Tuszynski, M.H., 2010. Extensive spontaneous plasticity of corticospinal projections after primate spinal cord injury. Nat. Neurosci. 13 (12), 1505–1510. https://doi.org/10.1038/nn.2691.
Ruppert, K.A., Nguyen, T.T., Prabhakara, K.S., Toledano Furman, N.E., Srivastava, A.K., Harting, M.T., Olson, S.D., 2018. Human mesenchymal stromal cell-derived extracellular vesicles modify microglial response and improve clinical outcomes in experimental spinal cord injury. Sci. Rep. 8 (1), 480. https://doi.org/10.1038/s41598-017-18867-w.

Saffen, D.W., Cole, A.J., Worley, P.F., Christy, B.A., Ryder, K., and Baraban, J.M. "Convulsant-induced increase in transcription factor messenger RNAs in rat brain." Proc. Natl. Acad. Sci. U.S.A. 1988; 85:7795–7799. doi: 10.1073/pnas.85.20.7795.

Saver, J.L., Fonarow, G.C., Smith, E.E., et al., 2013. Time to treatment with intravenous tissue plasminogen activator and outcome from acute ischemic stroke. JAMA 309, 2480–2488.

Skup, M., Gajewska-Wozniak, O., Grygielewicz, P., Mankovskaya, T., Czarkowska-Bauch, J., 2012. Different effects of spinalization and locomotor training of spinal animals on cholinergic innervation of the soleus and tibialis anterior motoneurons. Eur. J. Neurosci. 36, 2679–2688. https://doi.org/10.1111/j.1460-9568.2012.08182.x.

Souza, W.C., Conforto, A.B., Orsini, M., Stern, A., amp; André, C., 2015. Similar Effects of Two Modified Constraint-Induced Therapy Protocols on Motor Impairment, Motor Function and Quality of Life in Patients with Chronic Stroke. Neurol. Int 7 (1), 5430. https://doi.org/10.4081/ni.2015.5430.

Stonesifer, C., Corey, S., Ghanekar, S., Diamandis, Z., Acosta, S.A., amp; Borlongan, C.V., 2017. Stem cell therapy for abrogating stroke-induced neuroinflammation and relevant secondary cell death mechanisms. Prog. Neurobiol. 158, 94–131. https://doi.org/10.1016/j.pneurobio.2017.07.004.

Tigges, J., Gordon, T.P., McClure, H.M., Hall, E.C., Peters, A., 1988. Survival rate and life span of rhesus monkeys at the Yerkes regional primate research center. Am. J. Prima 15 (3), 263–273. https://doi.org/10.1002/ajp.1350150308.

Tigges, J., Nakagawa, S., Tigges, M., 1979. Efferents of area 4 in a South American monkey (Saimiri). I. Terminations in the spinal cord. Brain Res 171 (1), 1–10.

Tsang, Y.M., Chiong, F., Kuznetsov, D., Kasarskis, E., Geula, C., 2000 7. Motor neurons are rich in non-phosphorylated neurofilaments: cross-species comparison and alterations in ALS. Brain Res 861 (1), 45–58. https://doi.org/10.1016/s0006-8993(00)01954-5.

Vann, S.D., Brown, M.W., Erichsen, J.T., Aggleton, J.P., 2000. Fos imaging reveals differential patterns of hippocampal and parahippocampal subfield activation in rats in response to different spatial memory tests. J. Neurosci. 20, 2711–2718.

Vinet, J., van Weering, H.R., Heinrich, A., et al., 2012. Neuroprotective function for ramified microglia in hippocampal excitotoxicity. J. Neuroinflamm. 9, 27. https://doi.org/10.1186/1742-2094-9-27.

Wahl, A.S., Omlor, W., Rubio, J.C., Chen, J.L., Zheng, H., Schröter, A., Gullo, M., Weinmann, O., Kobayashi, K., Helmchen, F., Ommer, B., Schwab, M.E., 2014. Neuronal repair: asynchronous therapy restores motor control by rewiring of the rat corticospinal tract after stroke. Science 344 (6189), 1250–1255.

Weidner N1, Ner, A., Salimi, N., Tuszynski, M.H., 2001. Spontaneous corticospinal axonal plasticity and functional recovery after adult central nervous system injury. Proc. Natl. Acad. Sci. USA 98 (6), 3513–3518.

"What Is Stroke." Stroke.org, Americam Heart Association, 2018, www.stroke.org/understand-stroke/what-is-stroke/.

Wiessner, C., Bareyre, F.M., Allegrini, P.R., Mir, A.K., Frentzel, S., Zurini, M., Schnell, L., Oertle, T., Schwab, M.E., 2003. Anti-Nogo-A antibody infusion 24h after experimental stroke improved behavioral outcome and corticospinal plasticity in normotensive and spontaneously hypertensive rats. J. Cereb. Blood Flow. Metab. 23, 154–165.

Xian, P., Hei, Y., Wang, R., Wang, T., Yang, J., Li, J., Di, Z., Liu, Z., Baskys, A., Liu, W., Wu, S., Long, Q., 2019. Mesenchymal stem cell-derived exosomes as a nanotherapeutic agent for amelioration of inflammation-induced astrocyte alterations in mice. Theranostics 9 (20), 5956–5975. https://doi.org/10.7150/thno.33872.

Xin, H., Li, Y., Buller, B., Katakowski, M., Zhang, Y., Wang, X., Chopp, M., 2012. Exosome-mediated transfer of miR-133b from multipotent mesenchymal stromal cells to neural cells contributes to neurite outgrowth. Stem Cells 30 (7), 1556–1564. https://doi.org/10.1002/stem.1129.

Xin, H., Li, Y., Cui, Y., Yang, J.J., Zhang, Z.G., amp, Chopp, M., 2013. Systemic administration of extracellular vesicles released from mesenchymal stromal cells promote functional recovery and neurovascular plasticity after stroke in rats. J. Cereb. Blood Flow. Metab. 33 (11), 1711–1715.

Zai, L., et al., 2009. Inosine alters gene expression and axonal projections in neurons contralateral to a cortical infarct and improves skilled use of the impaired limb. J. Neurosci. 29, 8187–8197.

Zemke, A.C., Heagerty, P.J., Lee, C., Cramer, S.C., 2003. Motor cortex organization after stroke is related to side of stroke and level of recovery. Stroke 34 (5), e23–e28. https://doi.org/10.1161/01.STR.0000065827.35634.5E.

Zhang, B., Yin, Y., Lai, R.C., Tan, S.S., Choo, A.B., amp; Lim, S.K., 2014. Mesenchymal stem cells secrete immunologically active extracellular vesicles. Stem Cells Dev. 23 (11), 1233–1244.

Zhang, Y., Chopp, M., Liu, X.S., Katakowski, M., Wang, X., Tian, X., Zhang, Z.G., 2016. Extracellular vesicles derived from mesenchymal stromal cells promote axonal growth of cortical neurons. Mol. Neurobiol. 54 (4), 2659–2673. https://doi.org/10.1007/s12035-016-9851-0.

Zhang, Y., Chopp, M., Zhang, Z.G., Katakowski, M., Xin, H., Qu, C., Xiong, Y., 2017. Systemic administration of cell-free extracellular vesicles generated by human bone marrow derived mesenchymal stem cells cultured under 2D and 3D conditions improves functional recovery in rats after traumatic brain injury. Neurochem Int. 111, 69–81. https://doi.org/10.1016/j.neuint.2016.08.003.

Zhong, J., Liang, M., Akther, S., Higashida, C., Tsuji, T., Higashida, H., 2014. cfos expression in the paternal mouse brain induced by communicative interaction with maternal matesr. Mol. Brain 7, 66.